

# In-Situ Stress and Acoustic Logs Determined Mechanical Properties and Stress Profiles for Wellbore Stability Analysis in the Opuama Channel of the Niger Delta.

Abiodun M. Ajibade<sup>1</sup>, Olubola Abiola<sup>2</sup>, Pius A. Enikanselu<sup>2</sup>, and M. T. Olowokere<sup>2</sup>

<sup>1</sup> Department of Physical Science, Olusegun Agagu University of Science and Technology, Okitipupa, Ondo State, Nigeria

<sup>2</sup> Department of Applied Geophysics, Federal University of Technology, Akure, Ondo State, Nigeria.

**\*Corresponding author (e-mail [alongebiodun@gmail.com](mailto:alongebiodun@gmail.com))**

This study aimed to detect the overpressure and problems in the well that will be drilled based on exploration well data and determine the best conditions to minimize risks associated with wellbore stability. The objectives are to build a 3D pore pressure model for rock and estimate rock mechanical properties for wellbore stability analysis. Six (6) wells log and seismic data from AK Field of Niger Delta were used for the analysis. Geostatistical approach was used to build in-situ stress magnitudes and rock mechanical parameters from empirical relationship between density and velocity along 3D structural grid. Failure criteria were applied to for instability analysis. The final result will be a 3D pore pressure cube in the area based on quantitative analysis of post-stack seismic inversion. The results of the pore pressure analysis from the wells and the 3D pore pressure model indicate that top of overpressure occurs in the Akata Formation, then it is decreasing gradually approaching the hydrostatic pressure on Benin Formation. The mechanisms of overpressure are caused by under compaction, fluid expansion (kerogen maturation). The Akata Formation and Benin Formation are shale rocks so the type of mud weight that is well used is oil based mud (OBM). The result of this study can be used to predict minimum drilling mud pressure to drill safely and further prevent wellbore collapse and induced fracture in the study.

**Keywords:** In-situ stress; geomechanical properties; Mechanical Earth Model; borehole deformation; rock integrity; Geostatistics.

## Introduction

Accurate pore pressure estimation is needed in all aspects of oil and gas exploration and development. The subsurface pressure analysis is carried to determine the mud weight optimum. It is used to maintain the stability of the borehole which is influenced by the strain around it.

The ‘Bade’ Field is an onshore field located within latitude 5°30N to 5°40N and longitude 6°00E to 6°20E in the Niger Delta. It covers an area of 300 sq km. figure 1.

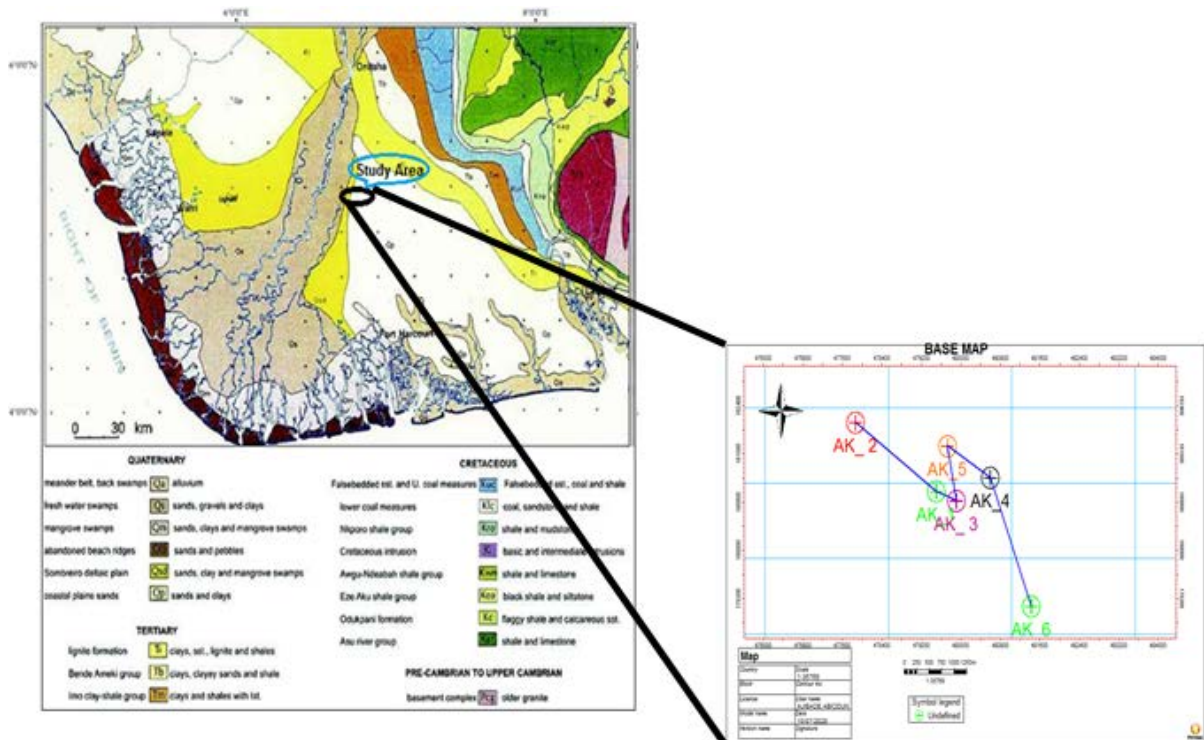


Figure 1: Geological map of the Niger Delta and surroundings (TJA Reijers), and Base Map of the study area

## Geological setting

Niger Delta province is the twelfth richest in petroleum resources, with 2.2% of the world’s discovered oil and 1.4% of the world’s discovered gas (Petro consultants, Inc. 1996a). The onshore portion of the Niger Delta Province is delineated by the geology of southern Nigeria and southwestern Cameroon (Fig.1). The northern boundary is the Benin flank--an east-northeast trending hinge line south of the West Africa basement massif. The northeastern boundary is defined by outcrops of the Cretaceous on the Abakaliki High and further east-south-east by the Calabar flank--a hinge line bordering the adjacent Precambrian. The offshore boundary of the province is defined by the Cameroon volcanic line to the east, the eastern boundary of the Dahomey basin (the eastern-most West African transform-fault

passive margin) to the west, and the two kilometer sediment thickness contour or the 4000-meter bathymetric contouring areas where sediment thickness is greater than two kilometers to the south and southwest.

### **Stratigraphy**

The Tertiary section of the Niger Delta is divided into three formations, representing prograding depositional facies that are distinguished mostly on the basis of sand-shale ratios. The type sections of these formations are described in Short and Stäuble (1967) and summarized in a variety of papers (e.g. Avbobvo, 1978; Doust and Omatola, 1990; Kulke, 1995).

Akata Formation as the base of the delta is of marine origin and is composed of thick shale sequences (potential source rock), turbidite sand (potential reservoirs in deep water), and minor amounts of clay and silt (Figs.3 and 4).

Overlying Formation is the deposition of the Agbada, which is the major petroleum-bearing unit, began in the Eocene and continues into the Recent (Fig. 3). The formation consists of paralic siliciclastics over 3700 meters thick (Fig. 4) and represents the actual deltaic portion of the sequence. The clastics accumulated in delta-front, delta-topset, and fluvio-deltaic environments. In the lower Agbada Formation, shale and sandstone beds were deposited in equal proportions, however, the upper portion is mostly sand with only minor shale interbeds.

The Agbada Formation is overlain by the third formation, the Benin Formation, a continental latest Eocene to Recent deposit of alluvial and upper coastal plain sands that are up to 2000 m thick (Avbobvo, 1978).

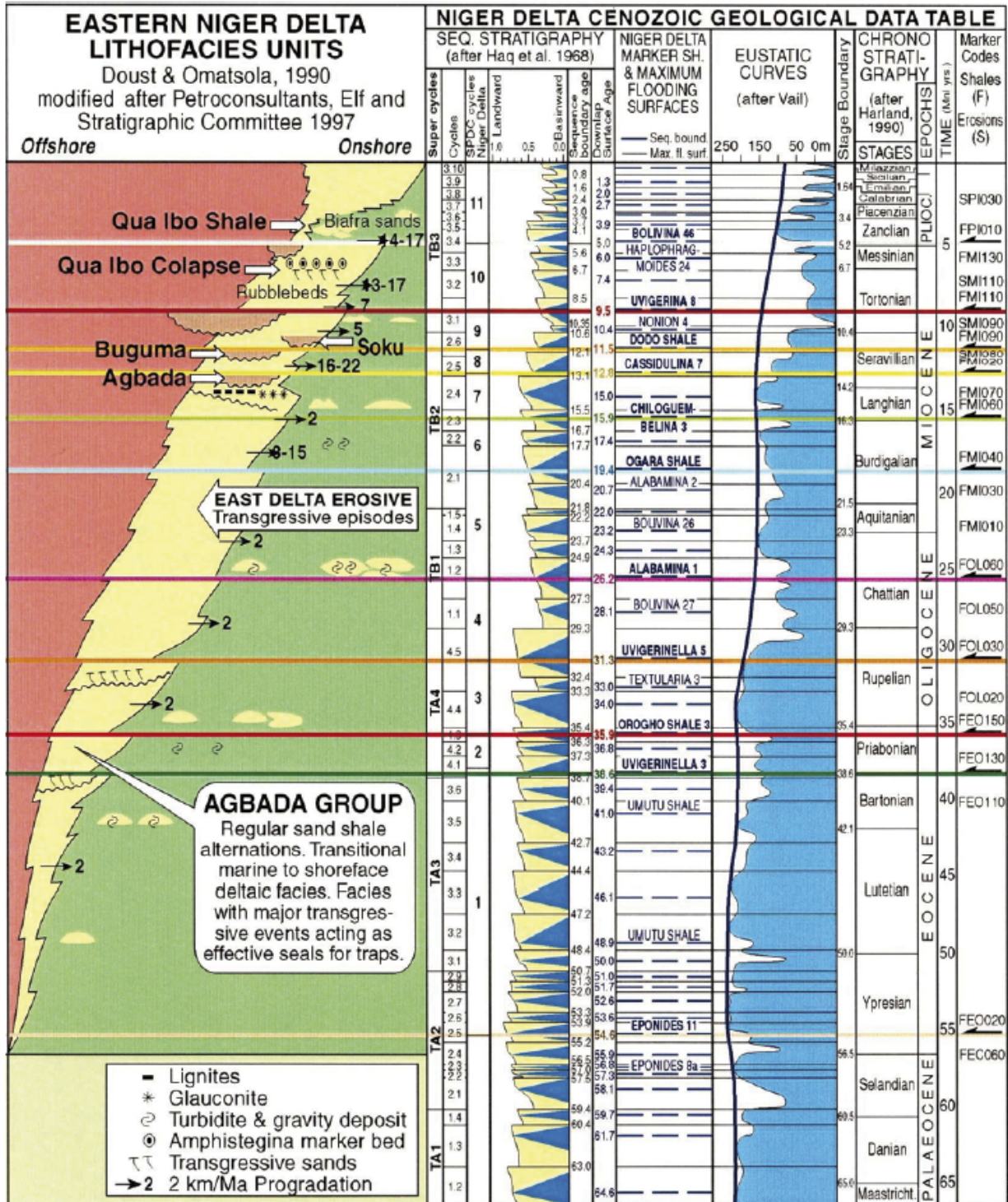


Fig. 3: Stratigraphic data sheet (east half) of the Niger Delta

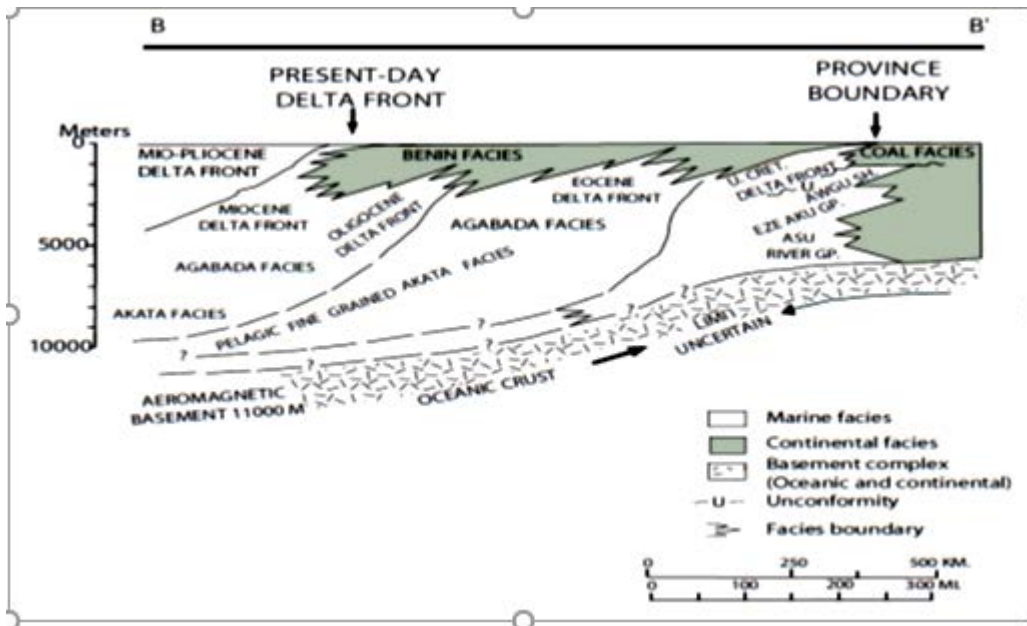


Fig. 4: Diagrammatic southwest-northeast (B-B') cross section through the Niger Delta Region. (modified from Whiteman,1982).

### Materials and Method of Data Analysis

The wells data used in this study are of total vertical depths that ranges from ~ 60.956955 m to 3013.640869 m. Six (6) wells log and 3D-seismic data within the study area were used build geomechanical model, and wellbore stability analysis within the study area. Specifically, gamma ray, sonic logs, and density logs were used for calibration while caliper, bit size, porosity, resistivity, spontaneous potential and caliper logs were used for quality control and lithologic correlation respectively. The interval of interest is from 2300m-2600m where there are available logging data for shale section.

### Method of Data Analysis

Checkshot and seismic data were equally used for the prediction. Faults were mapped on the basis of seismic expression and confirmed from available well logs. The well log, drilling and 3D seismic data were used to estimate in situ stress and rock mechanical parameters away from well. The in situ stress magnitudes and rock mechanical parameters models were built along the 3D structural grid, using the empirical relationship between density and velocity. These were treated as properties, upscaled and distributed along the 3D structural grid based on sonic interval transit time and density through a geostatistical approach. The existing 3D geological model, complete with structural framework, formation zonation, and petrophysical analysis were utilized to model the failure of rock analysis.

## Lithology Estimation from Well Logs and Seismic Data

Lithology units as shale and sands which form an essential pre-requisite for computing rock mechanical properties (elastic and inelastic) was identified and analyzed for velocity and interval travel time, because different relationships between dynamic and static moduli apply on different lithofacies.

## Rock Property Analysis based on Well Log Data

Mineralogy composition, porosity, permeability, volume of shale, and water saturation were analyzed as rock properties on all the available wells based on the lithofacies that will be defined throughout the entire section from surface to the base of the zone of interest.

## Computation of In-Situ Stress Magnitudes

Estimation of overburden stress, pore pressure, effective vertical stress and effective horizontal stress, fracture pressure is greatly required for failure studies. These were accurately determined from sonic and in-situ density logs for six wells. (Olowokere and Ojo, 2008a and 2008b).

The vertical stress at depth  $z$  is computed as the total weight of the overburden (Evans *et al.*, 1989 and Plumb *et al.*, 1991), where,  $\rho(z)$  = formation bulk density of overburden rocks as a function of depth,  $z$  and  $g$  = acceleration due to gravity.

Therefore, overburden stress ( $S_V$ ) was therefore computed by integrating formation density log data from the surface to the depth of interest. Horizontal minimum stress was calculated using, Eaton (1969) equation a physically based technique for determination of the least principal stress based on Poisson's ratio,  $\nu$ . The maximum horizontal stress was computed using the equation proposed by Peng and Zhang, 2007.

Magnitude of Overburden stress or Vertical stress ( $S_V$ ), Magnitude of Minimum horizontal stress ( $S_h$ ), and Magnitude of Maximum horizontal stress ( $S_H$ ) were estimated using Equation 1 – 3 below.

$$S_V = \int_0^Z \rho(z)gdz = \rho * g * z. \text{-----}1$$

$$S_h = \frac{\nu(S_V - P_p)}{1 - \nu} + P_p \text{-----}2$$

$$S_H = m * (S_V - S_h) + S_h \text{-----}3$$

where  $m$  is a constant, normally  $m = 0 - 2$ . In the normal faulting stress regime,  $m$  can generally be taken as 0.5

These parameters were determined in order to fully evaluate state of stress.

The magnitude of pore pressure gradient ( $P_p$ ) was calculated using Eaton’s **1975**, sonic equation relation at the true vertical depth of interest. Estimated pore pressure was used to compute the effective stresses by the theory of subcompaction. This is due to the facts subcompaction in shales could cause the porosity to remain high and a deviation of the normal compaction trend line in the sonic, resistivity and density data in a semi-log plot was noticed. This deviation from normal trend line was used to obtain  $\Delta T_n$  and  $\Delta T_0$  from sonic log data across five wells. The average values were then taken to compute pore pressure profile. Sonic, resistivity and porosity logs were used to predict Pore Pressure (top of overpressure) in the shale

- $P_{hd} = 1.07 * 0.052 * \text{Depth}$  ----- 4

- Pore pressure ( $P_p$ ) =  $S_V - (S_V - P_h) \frac{\Delta T_n^3}{\Delta T_0}$  ----- 5

Matthews–Kelly’s equation (1967) was used in the estimation of Fracture pressure (FP)

Fracture Pressure = (Mini Horizontal/Vertical Stress) \*(Vertical Stress -Pore Pressure) +Pore Pressure

- Fracture Pressure =  $(S_h/S_V) * (S_V - P_p) + P_p$  ----- 6

Where  $S_h/S_V = K_i$  known as matrix stress coefficient

**Effective Overburden Stress ( $S_V$ )**

External stress is not the only stress that has impart on the grains but also the impart of effective stress which includes pore pressure (Terzaghi, 1943). The effective stress is that part of the total external stress felt by the rock matrix.

$$\sigma_V = S_V - P$$
 ----- 7

So, biot’s parameter  $\alpha$  under Poro-elastic theory was used to relate pore pressure to effective stress of a porous media. For most practical applications,  $\alpha$  is close to 1. For partially saturated rocks, a modified form of Terzaghi, 1943 was obtained Biot, 1962

$$\sigma_V = S_V - \alpha P$$
 ----- 8

**Effective Horizontal Stress ( $\sigma_{hmin}, \sigma_{hmax}$ )**

Similarly, the effective horizontal stresses were determined from the relation below

$$\sigma_{hmin} = \sigma_{hmax} = S_h - \alpha P$$
 ----- 9

## Geomechanical Parameters Estimation

Rock properties in-terms of elastic and inelastic properties of the rock was modelled using rock features such as shale content, density and acoustic velocities based on geophysical well logging data (gamma-ray (GR), density ( $\rho_b$ ), sonic compressional transit time (DTc) and derived sonic shear transit time (DTs) logs).

Rock mechanical properties such as, Poisson's ratio ( $\nu$ ), internal friction angle ( $\phi$ ), cohesion (c) and uniaxial compressive strength (UCS or  $C_0$ ) were computed from the empirical relationships as provided by different authors and as applicable to rock failure analysis. Density and sonic logs was used to estimate elastic and inelastic properties of the rock for rock strength estimation. Relationship between shale content and velocity was established.

## Results and Discussion

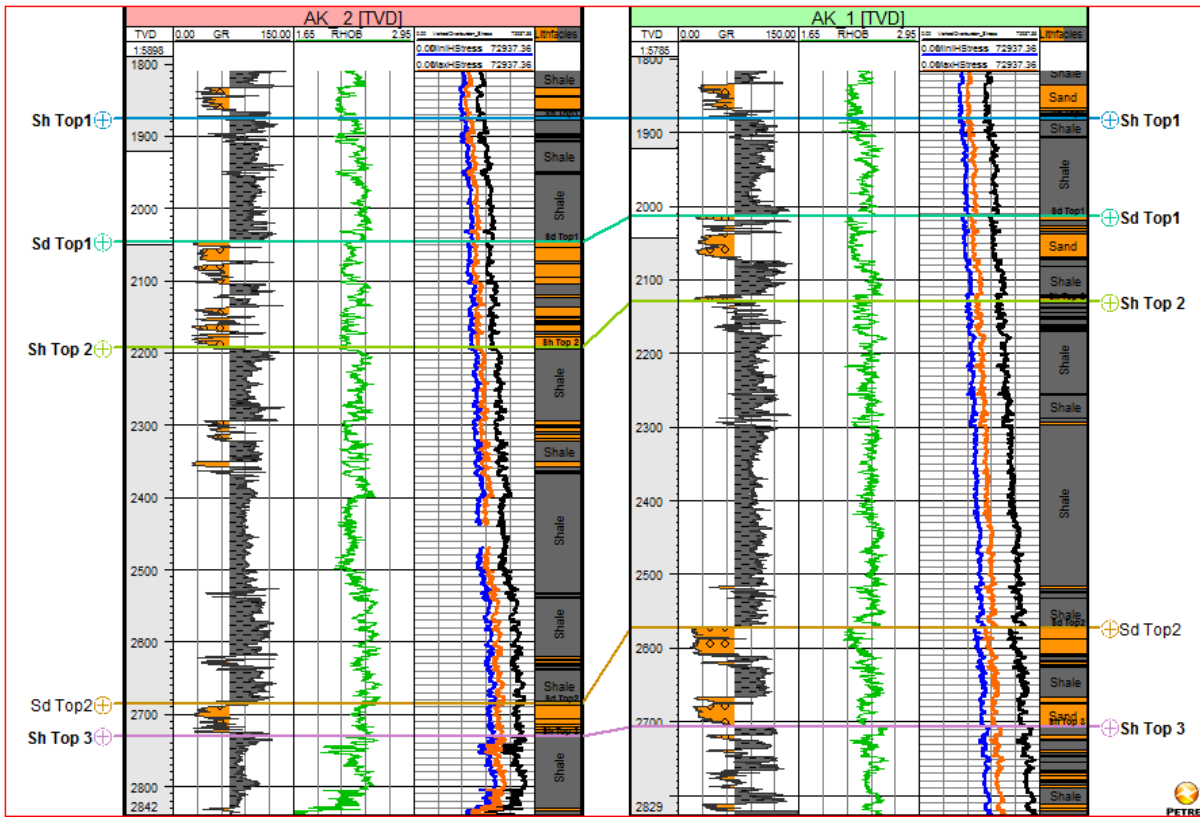
The interpretation stage requires putting together all the information and observations from various wells in a cohesive and meaningful way. For this report, data interpretation involves, firstly, evaluating the in-situ stress and geomechanical properties from sonic and density logs in all the wells. Secondly, zones of interest were detected and identified for rock integrity analysis.

### Estimated In-situ Stress Parameters Results

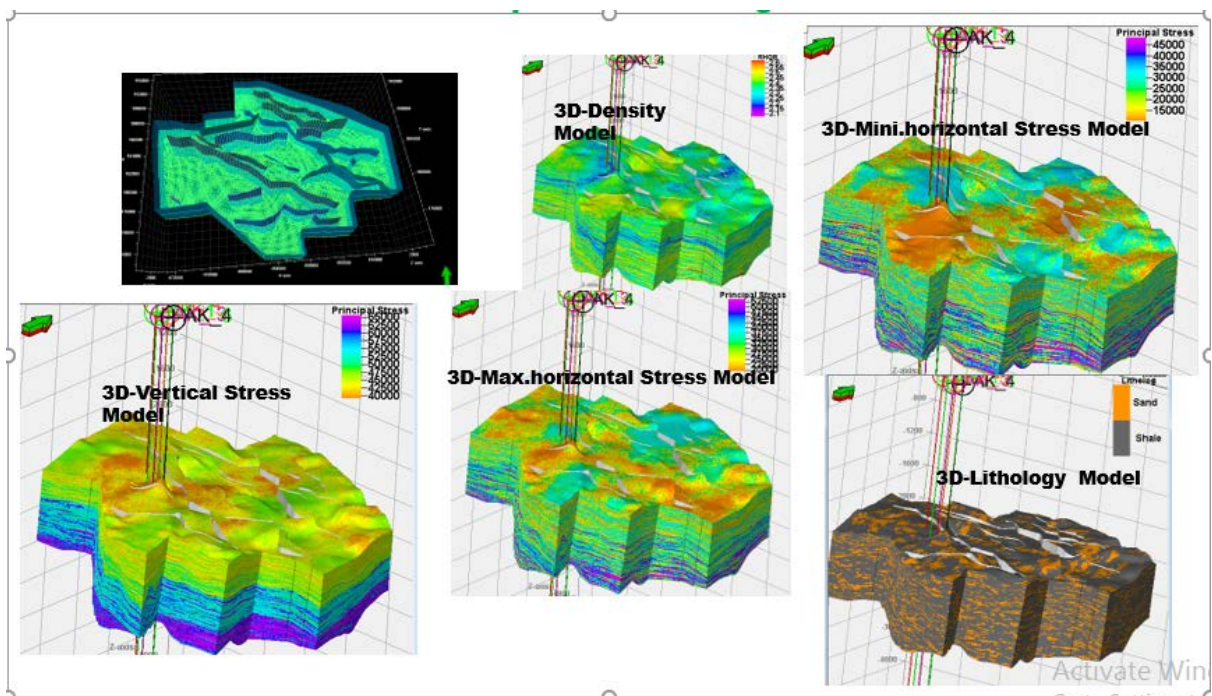
Gamma-ray, density and Overburden, maximum and minimum horizontal stress magnitudes profiles for Wells AK- 1 and 2 (Figure 5) showing that principal stresses is in order of  $S_v > S_H > S_h$  in all well "AK". The greatest stress here is vertical Overburden stress ( $S_v$ ), intermediate as Maximum horizontal stress ( $S_H$ ), and least stress is Minimum Horizontal stress ( $S_h$ ). This implies that, Fault regime within the study area is Normal fault according to Anderson, (1951). Magnitudes of the greatest stress is from (16054.85- 72937.36 pa), intermediate (6233.56-72937.36 pa) and least stress is from 5224.07- 51958.50 pa.

Figure 6a and 6b show the Density, Effective Stress Magnitude distribution and lithology Models within the rock volume and on the surfaces of the faults respectively. Integration of in-situ principal stress with seismic data to further examined the fault type (seismic section to generate 3D-view). Seismic section (inline 350), surface map and 3D-geo-model showed relative movement of rocks block to each other; as the faults intersect the surface from 2000m- 2400 and 2400m-2800m depth intervals which also confirmed Normal fault regime (Figure 6). The 3D geo-model showed lateral view of the magnitude of principal stress (Vertical,

Maximum horizontal and Minimum. Horizontal stress) increased with respect to depth due to effect of density and interval transit time properties (Figure 6a and b).



**Figure 5:** Gamma-ray, density and Overburden, max. and mini. horizontal stress magnitudes profiles (AK- 1 and 2)



**Figure 6a:** Density, Effective Stress Magnitude distribution and lithology Models

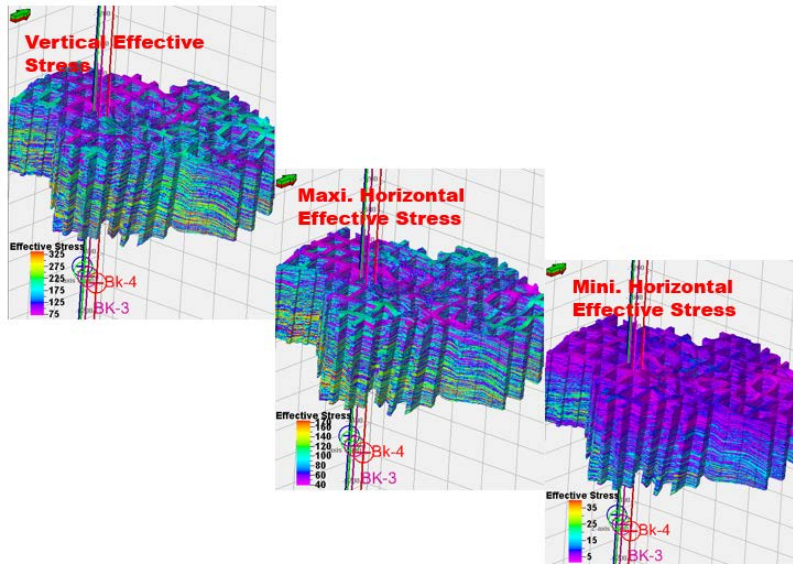


**Figure 6b:** Effective Stress Magnitude distribution on Fault surface Models

### Estimated Pore Pressure and Effective Stress

The stress imparts on the overburden rocks was determined by Estimating Vertical, Horizontal Effective stress, and pore pressure along the wellbore. Biot’s 1962. It showed that they increase with respect depth within the shale formation with horizontal effective stress being the least but decrease within sand, Changes in Pore pressure has led to observed changes in stresses magnitude acting on shale formation and the reservoir rock(sand) ( Figure 7 and 8).

Estimated effective stress (Vertical, and Horizontal) along the wellbore show their impart on the overburden rocks as a result of  $P_p$  and biot constant (Terzaghi, 1943 and Biot, 1962.).  $P_p$  increase in well AK-1 and 2, cause the observed decrease in effective stress. In ak-3 and 4 decrease in  $P_p$  caused the effective stress to increase in magnitudes of  $P_p$  and biot constants decrease was due to porosity, permeability, grain to grain contacts and unloading of sediments resulting to an increase in stress magnitudes.

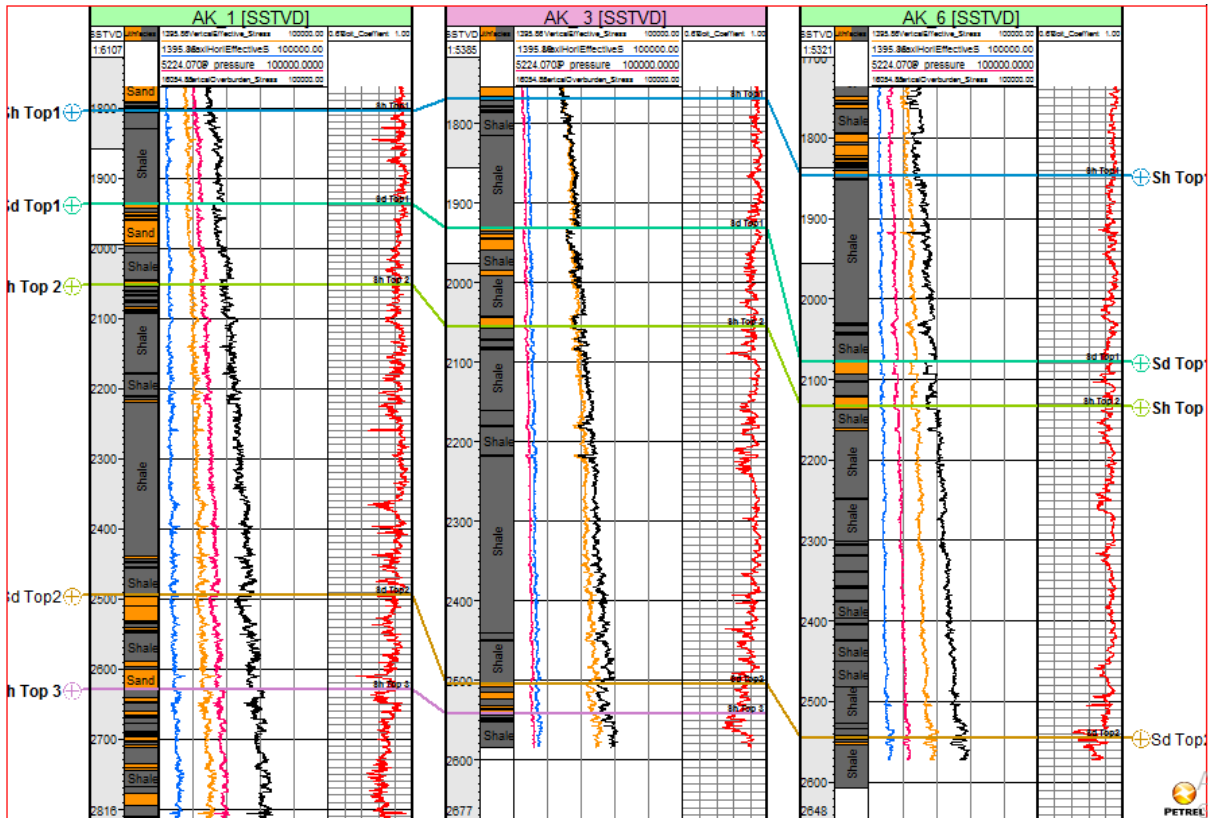


**Figure 7:** Overburden stress, Pore pressure and Effective stress (horizontal and vertical) Profiles

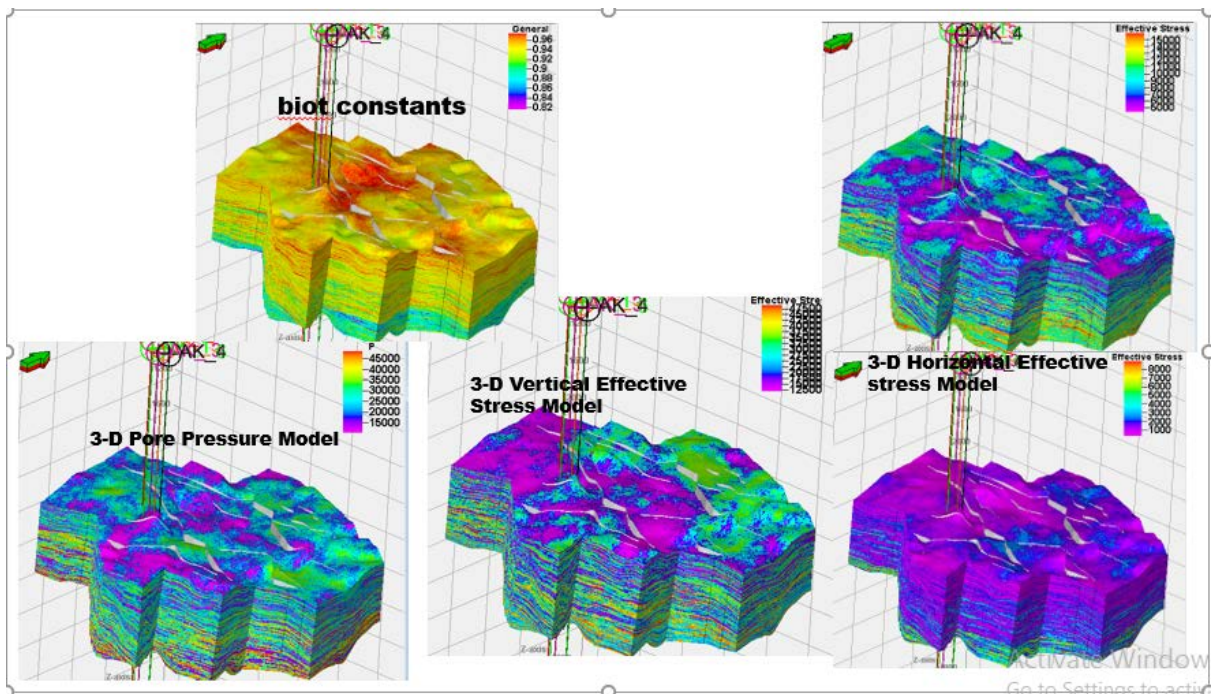


**Figure 8:** 3D-models of Effective stress (horizontal and vertical) and pore pressure

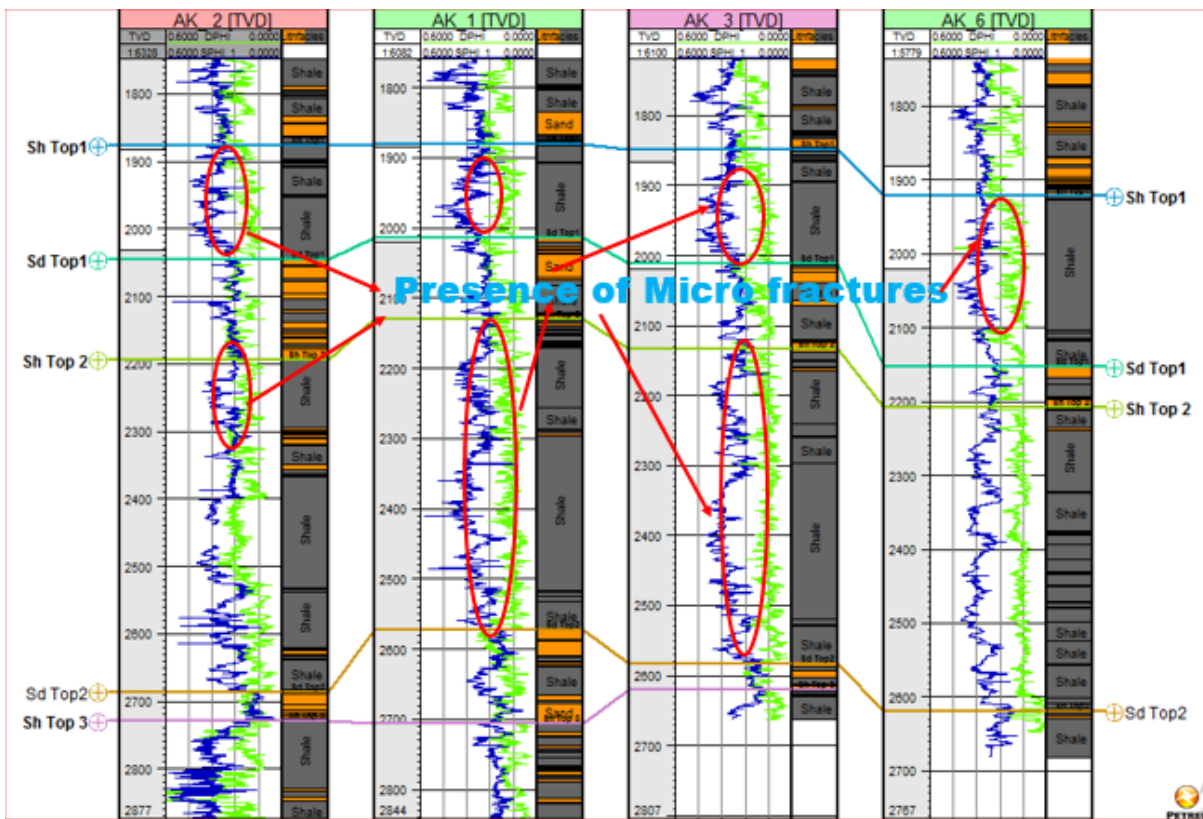
### Sonic and Density Porosity Log Analysis

Figure 9 shows the Sonic and density porosity logs and litho-facies panel for 4-AK wells.

Sonic and density porosity logs signatures further confirmed the presence of weak and micro-fracture within shale formation. Observing the crossing over between high sonic against low density porosities. The open gaps between them gave an indication of micro-fractures and this made the formation to experienced caving/spalling off of sediments from weak sediments around the wellbore (Figure 9).

Integration of unconfined compressive strength (UCS) with geophysical well logs along wellbore, revealed that high porosity, low velocities, elastic moduli, and rock strength within the shale formation had given room for presence of micro-fractures in this formation. The observed porosity from sonic log is secondary porosity due to the applied stress (Olowokere 2008).

The porosity values ranges from 0.24-0.39 and this, made shale strength to be lower than that of sand. Since high magnitude of in-situ stress was confirmed within shale formation against low rock strength leading easy fracturing of the formation.



**Figure 9:** Sonic and density porosity logs and litho-facies panel for 4-AK wells

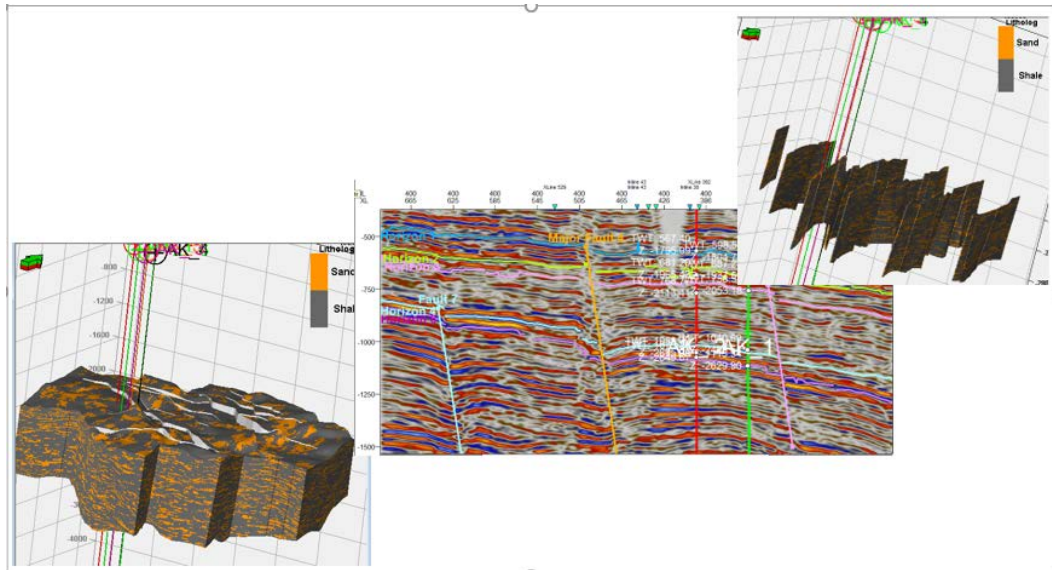


Figure 10: displayed of wells and faults on seismic section and 3D-lithofacies model

### Rock Strength Evaluation

Figure 11 shows the Unconfined Compressive Strength and Cohesion with coefficient of frictional angle Variation on Fault Surface Models. The magnitude of unconfined compressive strength (UCS), cohesive strength and coefficient internal friction angle were very low compared to the reservoir sand counterpart along wellbore and 3D models within the study area (Figure 11). These showed that shale formation had undergone degradation as results of weathering process (wetting and drying cycles) weaken this zone and result to low strength. The observed zone of interest is from 2200m to 2600m depth for shale formation in all the wells and laterally from 3D models.

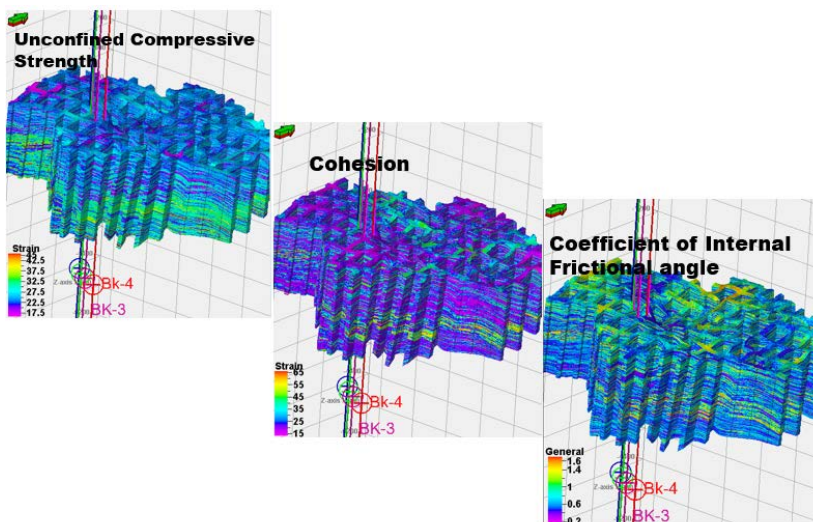


Figure 11: Unconfined Compressive Strength and Cohesion with coefficient of frictional angle Variation on Fault Surface Models

## Conclusion

Geophysical well logs with available information from four wells and 3D seismic data were used for rock strength and integrity study. Mathematical relationships were used to accurately estimate in-situ stress and mechanical parameters. The magnitudes of the In-situ principal stress (overburden, maximum and minimum Horizontal) increase with respect to the lithology and the density variation. Stress magnitudes for the reservoir sand are lower than that of the shale formation irrespective of their depositional depth in the study area. The rock mechanical parameters revealed that reservoir sand has higher magnitudes than shale formation.

The results of 3D models imaged the distribution of in-situ stress, and rock mechanical parameters to the surrounding in the study area when treated as properties to view their lateral variation for failure analysis. These showed that the shale formation is not strong enough for the encountered high stress magnitudes. And these explained displacement of rock units from seismic section and generated 3D litho-facies model, revealing the possibility of wellbore or rock failure in the study area due to instability from underbalanced of the overburden sediments.

## REFERENCES

- [1]. **Alkamil, E.H.K., Abbood, H.R., Flori, R.E. and Eckert, A., 2017.** Wellbore Stability Evaluation for Mishrif Formation. Paper Presentation at the SPE Middle East Oil & Gas Show and Conference, Bahrain, pp. 1-15.
- [2]. **Avbovbo, A. A., 1978.** Tertiary lithostratigraphy of Niger Delta: *American Association of Petroleum Geologists Bulletin*, vol. 62, pp. 295-300.
- [3]. **Babatunde A. Salawu, Reza Sanaee, and Olumayowa Onabanjo (2017).** Rock Compressive Strength: A Correlation from Formation Evaluation Data for the Niger Delta\* Search and Discovery Article #30488 (2017) \*\*Posted February 20, 2017
- [4]. **Barton, N. R., 1973.** Review of a New Shear Strength Criterion for Rock Joints. *Engineering Geology*, Vol. 7, pp. 287-332.
- [5]. **Biot M. A., 1941.** General theory of three-dimensional consolidation. *J Appl Phys* 12(1): pp155-164.

- [6]. **Biot, M.A., 1962.** Mechanics of deformation and acoustic propagation in porous media. *Journal of applied physics*, 33(4), pp.1482-1498.
- [7]. **Bradley W.B. 1974.** Borehole Failure Part 1: Failure of Inclined Boreholes, Technical Progress Report BRC-EP 18-74-P, Shell Bellaire Research Center, Houston, October 1974.
- [8]. **Burke, K., 1972.** Longshore drift, submarine canyons, and submarine fans in development of Niger Delta: *American Association of Petroleum Geologists, Bulletin* vol. 56, pp. 1975-1983.
- [9]. **Chang, C., Zoback M. D., & Khaksar, A., 2006.** Empirical relations between rock strength and physical properties in sedimentary rocks: *Journal of Petroleum Science and Engineering*, 51, 223–237.
- [10]. **Doust, H., and Omatsola, E., 1990.** Niger Delta, in, Edwards, J. D., and Santogrossi, P.A., eds., *Divergent/passive Margin Basins*, AAPG Memoir 48: Tulsa, American Association of Petroleum Geologists, Bulletin, pp. 239-248.
- [11]. **Eaton, B.A. (1975).** The equation for geopressure prediction from well logs. SPE, Paper No. 5544, 11P.
- [12]. **Evamy, D.D.J., Haremboure, P., Kamerling, W.A., Knaap, F.Molloy, A. and Rowlands, M.H., 1978.** Hydrocarbon habitat of the Tertiary Niger Delta. *American Association of Petroleum Geologists Bulletin* 62, pp. 1–39.
- [13]. **Fidelis A. A. and Akaha C. T., 2016.** Geomechanical Evaluation of an onshore oil field in the Niger Delta, Nigeria. *IOSR Journal of Applied Geology and Geophysics (IOSR-JAGG)*, e-ISSN: 2321–0990, p-ISSN: 2321–0982. Volume 4, Issue 1 Ver. I (Jan. - Feb. 2016), pp. 99-111. [www.iosrjournals.org](http://www.iosrjournals.org)
- [14]. **Fjaer, E. Holt, R. M. Horsrud, P. Raaen, A. M. and Risnes, R., 1992.** *Petroleum Related Rock Mechanics*, 2<sup>nd</sup> edition, Vol.53, Amsterdam, Elsevier Publications, 1992.
- [15]. **Jaeger, J. C., and N. G. W. Cook. 1976.** *Fundamentals of Rock Mechanics*. Chapman and Hall, London, 585 P.
- [16]. **Kingsley Nwozor and Gareth Yardley, 2015.** Overburden Stress Estimation: A New Model for the UK Sector of the Central North Sea. Department of Geology and Petroleum Geology, University of Aberdeen, UK .Email: [kknwozor@abdn.ac.uk](mailto:kknwozor@abdn.ac.uk). AAPG ICE Melbourne, Australia. September 2015

- [17]. **Kulke, H., 1995.** Regional Petroleum Geology of the World. Part II: Africa, America, Australia and Antarctica: Berlin, Gebrüder Borntraeger, pp. 143-172.
- [18]. **Lehnerand De Ruiter, P.A.C., 1977.** Structural history of Atlantic Margin of Africa: *American Association of Petroleum Geologists Bulletin*, v.61, pp. 961-981.
- [19]. **Olowokere M. T. and J.S. Ojo, 2008a.** Application of compaction trends in the prediction of porosity distribution in ‘Weden Field’, Niger Delta, Nigerian. *Journal of Mining and Geology (JMG)*, Vol. 44, (2) pp. 161-171.
- [20]. **Olowokere M. T. and J. S. Ojo, 2008b.** Application of travel-time inversion in velocity anisotropy estimation for lithology discrimination in some parts of the Niger Delta, *Nigerian Journal of Mining and Geology (JMG)*, Vol. 44, (2) pp. 173-182.
- [21]. **Olowokere M. T., 2008.** Stratigraphy, Facies Distribution and Depositional History of the Niger Delta shelf Margin. *Journal of Mining and Geology (JMG)*, Vol. 44, (1) pp. 57-69 .
- [22]. **Short, K.C. and Stauble, A.J., 1967.** Outline geology of the Niger Delta. *American Association of Petroleum Geologists Bulletin* 51, pp. 761–779.
- [23]. **Stacher P., 1995.** Present understanding of the Niger Delta hydrocarbon habitat, in: M.N. Oti, G. Postma (Eds.), *Geology of Deltas*, Balkema, Rotterdam, 1995, pp. 257-268.
- [24]. **Whiteman, A., 1982.** Nigeria: Its Petroleum Geology, Resources and Potential: London, Graham and Trotman. 394P.
- [25]. **Wyllie, M.R.J., Gregory, A.R. and Gardner, G.H.F., 1956.** Elastic Wave Velocities in heterogeneous and Porous Media, *Geophysics*, 21 (1), pp. 41-70.
- [26]. **Yu, J.H.Y. and Smith, M., 2011.** Carbonate Reservoir Characterization with Rock Property Invasion for Edwards Reef Complex, the 73rd EAGE Conference and Exhibition incorporating SPE Europe, 23 -26 May, Vienna, Austria, 346-350.
- [27]. **Zhang John J. and Laurence R. Bentley 2005.** Factors determining Poisson’s ratio. CREWES Research Report — Volume 17 (2005)
- [28]. **Zhang L, Cao P, and Radha KC., 2010.** Evaluation of rock strength criteria for wellbore stability analysis. *Int J Rock Mech Min Sci.*;47: pp. 1304–1316.
- [29]. **Zoback MD et al., 2003.** Determination of stress orientation and magnitude in deep wells. *Int J Rock Mech Min Sci* 40:pp. 1049-1076.